Development and test of two high power conventional pulsers for radiography application

Frédéric Bayol, Anthony Coe, Clément Gaston, Patrick Mouly, Arthur Piaser, Kévin Van de Wiel, Mathieu Vaurs,
ITHPP
Thégra, France
fbayol@ithpp-alcen.fr

Aled Jones, Matt Evans, John Haynes, James Rutledge, Phil Williams
AWE
Aldermaston, United Kingdom

***Abstract*— This work concerns the development and testing of 2 radiography pulsers (~2MV, 650kA, ~100ns) to enhance the hydrodynamic testing capabilities of the Atomic Weapons Establishment (AWE) in Aldermaston (UK). The generators have to fire on a Plasma Filled Rod Pinch diode (PFRP) to provide two ultra-bright X-ray sources on 2 radiography axis separated by 45°. The design uses a high voltage high-energy 20-stage balanced Marx charged up to +/-100kV. It uses specifically developed switches operating under pressurized dry air. The machines do not use any SF6. This Marx is fired with a small jitter to charge a ~50ns deionized water Pulse Forming Line (PFL) up to an operating voltage of ~4.3MV (at +/-90kV Marx charge). The discharge of this line occurs thanks to a multi-channel triggered oil switch providing a low inductance and associated fast switching. The ~100ns width pulse generated is transmitted by a water transmission line to a vacuum chamber using a radial monolithic interface. This output is similar to the Naval Research Laboratory Gamble II generator on which was developed and tested the AWE's PFRP diode. Initially, the generator fired on a resistive load prior to using a Large Area Diode (LAD) providing the ~3Ohm expected impedance. The Marx tank has a hydraulically operated side door under which the Marx can slide out and hang for ease of assembly and maintenance. So, the 2 machines have a handed design to accommodate their installation in a refurbished building. The general electrical and mechanical design of these generators, as well as the main problems encountered during the testing phase, have already been presented in [1]. This publication will therefore just remind the definition of the system and focus on the latest optimizations and results of the 2 machines, both on the resistive load and on the LAD. The operation of the main oil switch will also be described in detail.**

Keywords—component: flash-radiography, Marx, Pulse Forming line, Large area diode, conventional pulser, oil switch, radial interface.

I. INTRODUCTION

AWE wants to improve its hydrodynamics testing capabilities by the use of 2 flash-radiography pulsers (~2MV, 650kA,~100ns) firing on Plasma Filled Rod Pinch diodes (PFRP). Following a competitive tender launched in 2016 ITHPP was chosen for the development of 2 conventional pulsers (preferred to an alternative proposed solution with LTD) at the beginning of 2018.

II. REQUIREMENTS AND PRELIMINARY DEFINITION

The main requirements for the machine were to provide a peak positive output voltage of 2MV into a 3Ω load and to be operable between 1 to 2MV. The pulse length had to be <100ns ($80\%\ of\ \int V^2 . \mathrm{dt}$), and >80ns. The current prepulse on the short-circuit load must not exceed 20kA. A high reproducibility better than ± 5% was requested with a total jitter < 50ns 1σ (for synchronisation with the PFRP plasma injection). A failure rate lower than <1/200 was also expected. In terms of mechanical constraints, the output axis height had to be at 1.4m with a movable machine for diode refurbishing. A precision for the positioning of the X-ray source better than ±1mm in all direction was asked for and a LAD diode for testing at 1 shot/h had to be provided (shot rate of 1 shot/day minimum for the PFRP). In terms of operations, the machine was to be remotely controlled and operable by 2 people, with limited maintenance requirements and high availability. Finally, the environmental impact had to be minimised as much as possible (i.e. no SF6).

The main architecture uses a Sandia ZR-style ±90-95kV balanced Marx charging to 4.3MV a 3Ω, 50ns transit time water insulated PFL. A multi-channel triggered oil switch derived from the Gamble II machine at the Naval Research Laboratories (NRL) [2] discharges the coaxial line. The output pulse is then transmitted thanks to a water insulated 3Ω, 40ns Transmission Line (TL) to a vacuum chamber. The end section of the machine is also very similar to the Gamble II machine in order to limit the risk at the integration of the PFRP that was developed initially by NRL and AWE on this same machine. It uses a low inductance monolithic radial interface. The main disadvantages of such a solution is that the output performances are strongly linked to the switch operation that should close with multi-channelling to provide reduced inductance and resistance and get the required output characteristics.

III. ELECTRICAL DEFINITION

Simplified electrical schematics were initially used to simulate the whole generator operating on the different types of load: a resistive one, a LAD or the PFRP with its dynamic impedance varying between a short for 20-30ns and rising to 2-3Ω for ~100ns before collapsing again. It used an equivalent RLC model for the Marx with a series inductance deduced from the scaling of data given in the bibliography for the ZR Marx and other machines. This is followed by an output series resistance and diverter branch, the PFL, a single gap model for the oil switch, the TL, and all the possible loads (fixed resistance, LAD or PFRP) as shown on the Fig. 1.Looking at existing machines and results, it was shown that the use of physical resistive models for the switches (in the Marx and in oil), was indeed mandatory in order to get reliable and possibly predictive simulations. The key component in this architecture is the multi-channel triggered oil switch as shown with the

Work under contract n° 30411512

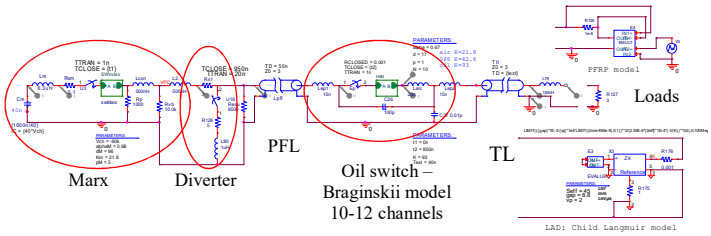

Fig. 1. First simplified model for the generator

Gamble II geometry in Fig. 2. A disk with a floating voltage typically placed at 1/3 of the distance between the hot PFL electrode and the cold TL one. With the first closure of the axial trigger gap, its potential relatively to the cold electrode is raised to a value higher than the PFL charge thanks to the ringing effect created by the central inductor. The large gap 2 then closes and, in sequence, the small gap 3. Thanks to these fast voltage changes, limited by the parasitic capacitance of the disc and the series inductance, multiple channels (>10) are generated on both gaps providing a low series resistance and inductance for the main discharge circuit (typically <50nH for the full arcs and switch electrodes section).

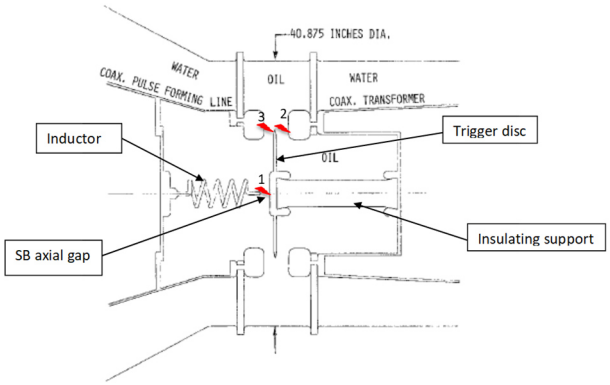

Fig. 2. Principle of operation of the Gamble II oil switch

The main risk with our proposed design compared to the Gamble II machine is that the suppression on the Intermediate Store (IS) generates a higher stress on this switch that has to hold the voltage for a much longer time (charging time of the PFL increased from ~160ns to more than 800ns) but still with the need of getting efficiently triggered. Despite this, the configuration was chosen as it was more compact and efficient. Fig. 3 presents some results of the first simulations done during the definition phase showing the requirements could be reached (whilst maintaining a margin on the Marx charge voltage).

IV. Overall Mechanical Design

The overall mechanical design of the machine is shown at Fig. 4. The oil tank has been equipped with a side door, movable by two large hydraulic actuators and on which the whole Marx (or individual columns) can slide in and out on to facilitate assembly and maintenance. The overall dimensions of the machine, on which are also embedded the subsystems (water and oil treatment systems, vacuum group…) to facilitate its movement, are 9m long, with a width (with the door opened) of 6.3m and a height of 4.6m.

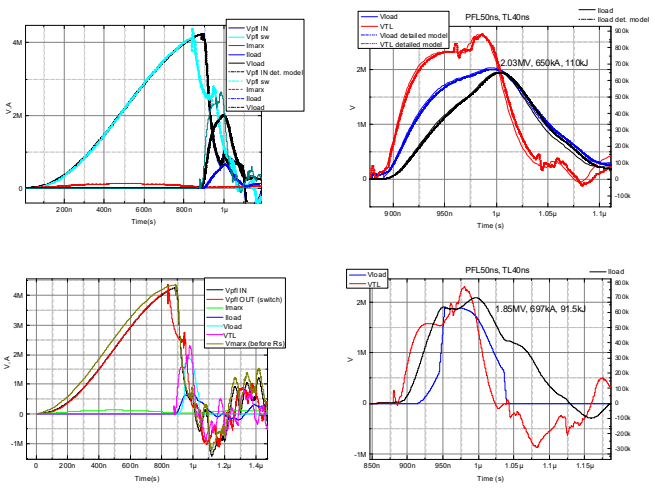

Fig. 3. First simulation results on a LAD (top, first initial model compared to a second one a bit more detailed) and on the PFRP (bottom)

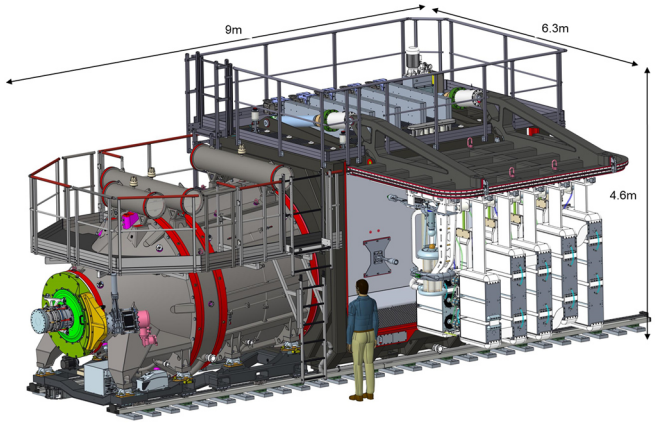

Fig. 4. Overall design of the generator with Marx hanging on the opened side door

The total weight of the pulser including its fluids is ~70t. The 40 General Atomics C32979 capacitors (100kV, 1.6µF) are arranged in five rows (10/8/8/8/6 repartition) to optimize the breakdown length along the polyethylene hangers on the top that increase with the discharge voltage of the Marx. The rows can be moved individually or together. Automatic connections / disconnections are used for the Marx (towards ground and to the PFL, trigger and charging ones), so entering the tank is not required. The Marx is routinely charged to +/-90kV (tested up to +/-100kV) and discharged thanks to 20 specifically developed switches, operating with pressurized dry air (up to ~10 bars). The triggering is done thanks to a 10-stage ±50kV mini-Marx delivering ~500kV to a trigger bar on the first row of the Marx. It is placed on the back wall of the tank and can also slide on rails for easy insertion and removal for maintenance. Two mechanical clamps (blockers from Hänchen) are on the door actuators to provide a redundant safety feature in addition to the counterbalance valves that prevent any possible accidental depressurization of the actuators. All the caps are equipped with an individual pneumatically actuated short-circuiting arm that closes with the help of the weight and a spring (fail safe design). The +100 and -100kV charging bars, that distribute the voltage to the caps using liquid resistors, are

manufactured in sections with spring actuated contacts. This facilitates the splitting of the rows, moved by electric motors with a position encoder and a chain system. A visual check of the position of these short-circuiting bars is sufficient to guarantee the possibility of safe intervention.

The mechanical design was supported by numerous 2D and 3D electrostatic calculations using the ANSYS/Maxwell software to look at critical points and define the highly stressed areas. Breakdown risks were analyzed either in water or oil using well-known breakdown criteria to define the main dimensions and geometries of the lines and oil switch section. The conception was also sustained by many Finite Element Model (FEM) mechanical calculations also done with the ANSYS suite. These allow to access the constraints repartitions in the materials and check sufficient margins exist. The possible flexing are also inferred under the fluids hydrostatic pressures and own weight of the parts. An interesting calculation to highlight is the one done to look at the maintenance configuration with the Marx hanged under the opened door. Fig. 5 presents on the left the results of the calculation with 1.25x overload considered on the Marx weight (5.75t instead of 4.5t) showing 190MPa max. Von Mises equivalent stress and a 5mm flexing in the middle of the door. This flexing is in very good agreement with the experiment done during the mechanical factory acceptance testing as shown on the right pictures (using concrete blocks for the loading and measurement thanks to a telemeter). The measurement of flexing measured in the middle of the door (~5.5mm) and on one corner (~4.5mm) confirmed the reliability of these calculations for the different cases studied. The fact the door returns to its initial position after the unloading also confirms this deformation corresponds to an elastic one only.

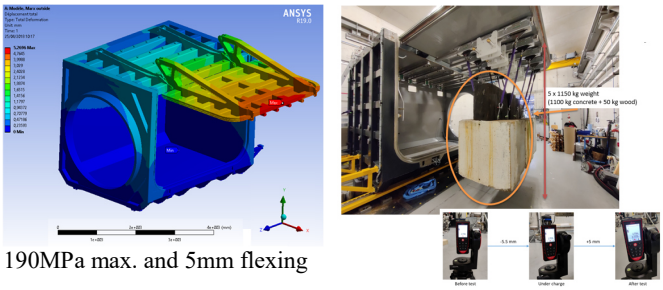

Fig. 5. Comparison of the calculation (left) and experiment (right) on the opened door with 5.75t overload

The calculations on the oil/water and water/vacuum interfaces also confirmed that it was possible to open for example the generator at the switch location without needing to drain all the fluids in the pulser that can facilitate and fasten its maintenance. The design of the vacuum interface has been a bit tricky as the use of a monolithic radial interface, moreover in positive polarity, is not very usual. The classical breakdown criteria that apply to segmented interface with 45° bevel insulating rings are not adequate (and not fulfilled if applied). The geometry has therefore been defined comparatively to the proven geometry of Gamble II despite of the fact we have chosen to use Rexolite™ (instead of a molded polyurethane with a Dendresist coating) to improve the mechanical resistance, the behavior under vacuum and to eliminate the need to develop a coating material similar to this proprietary preparation. Despite an initial careful design, some breakdowns of the interface have been observed during the first tests that lead to an increase of the distance between the interface and the chamber wall/door, and a re-shape of its geometry, in order to reduce the electric field on that surface. Indeed, it seemed from different tests that an effect linked to the electronic emission at this location seem to be responsible of these breakdowns.

Finally, a LAD was defined. To limit the risk of impedance collapse due to plasma expansion for this low operating impedance of ~3Ω that would have led to the use of a small gap, we have chosen to operate the MITL in self-limited regime with a stable impedance given by the anode center conductor diameter (with a large gap at the end of the line). We have also studied the electron transport with the LSP PIC code and have defined a specific geometry of the graphite anodes placed at the end of the positive center conductor to limit the energy deposition on the material, prevent material damages and allow multiple successive shots.

V. Tests Results

We have experienced a significant number of birth faults but we quickly obtained a very good operation of the whole chain μ-Marx/mini-Marx/Marx with limited jitter (<6ns 1σ, given mainly by the μ-Marx) and very good reproducibility despite of the very simple triggering scheme of the first row only. Fig. 6 presents a set of shots with increasing charge voltage on the Marx from 40 to 100kV. Also, the oil switch proved to be able to withstand the longer PFL charging time (using 185-190mm gap) without self-breaking and to close with multi-channeling (>10 channels) when correctly triggered. Fig. 7 presents an example of a first series of shots on the resistive load and with a ± 90kV charge on the Marx. A fast rising front can be observed on the output voltage that confirms the very efficient switching with multi-channeling. The overall jitter over these 9 consecutive shots was 85ns and is mainly linked to the jitter of the trigger switch. Different geometries of the trigger electrodes have been tested to improve it and the typical min-max jitter obtained over a large number of shots with the same configuration is around 100-150ns. As the number of channels tends to reduce with the charging voltage, e.g. at ~185mm gap, good operation is obtained between 70 and 90kV only.

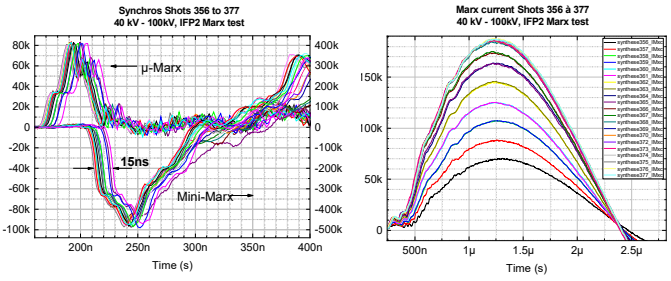

Fig. 6. Typical results of the trigger system (left) and Marx current output (right) from ±40 to ±100kV charge (Marx alone firing on the series + diverter resistors = ~7.5Ω)

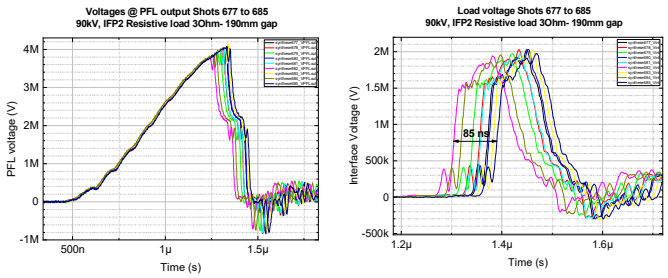

Fig. 7. Example of a consecutive series of 8 shots at 90kV charge on the resistive load (left: voltage at the output of the PFL, right: voltage measured on the interface in water)

At 60kV, bad closure can be observed on some shots with possible strong degradation of the output pulse (decrease of the max.voltage and increase of the pulse width that become more triangular). Comparison of shots from 90 down to 60kV charge are shown on the left graph of Fig. 8. A progressive decrease of the rising front quality may be seen between 90 to 70kV. An opened shutter image taken with a fisheye allowing to distinguish the full circumference of the oil switch allows to very easily distinguish the numerous channels (at least in the foreground) distributed on both sides of the trigger disk placed at ~1/3 of the gap distance toward the PFL side. After some little geometry adjustments, we have also obtained a good operation of the LAD with the possibility to make consecutive shots without any refurbishing. Fig. 9 presents a series of 11 consecutive shots at 90kV, synchronized in time, that also allow to verify the good reproducibility of the generator. The peak voltage on the diode reach 2-2.2MV for a current in vacuum of ~570kA. This current is measured by a rogowsky coil on the outer MITL conductor and therefore corresponds to a cathode current excluding the vacuum current flow, that should be around 5-10% according to the simulations and current measurement in water. The max. power delivered to the load (with voltage on the diode calculated thanks to an inductive correction) reaches 1.2TW for a delivered energy of 95kJ (so, the transfer efficiency is around 37-40%). The possibility to successfully shoot the pulser directly at 90kV after a full refurbishing of the interface and vacuum chamber has also been checked as it is the way it will have to be used with the PFRP that is destroyed at each shot and generates strong pollution.

During the definition phase and progression of the mechanical design we have also detailed our electrical model of the full

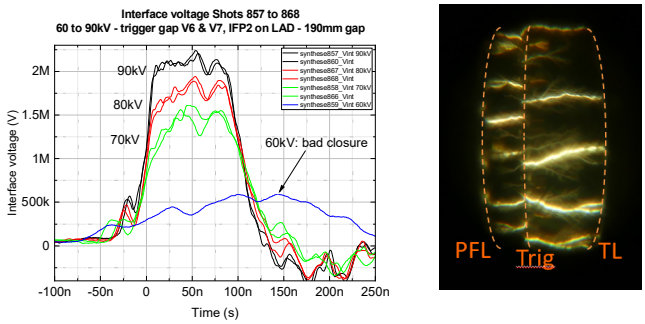

Fig. 8. Interface voltage (synchronized in time) between 90kV and 60kV (left) and open shutter picture of the switch arcs taken with a fisheye at 90kV

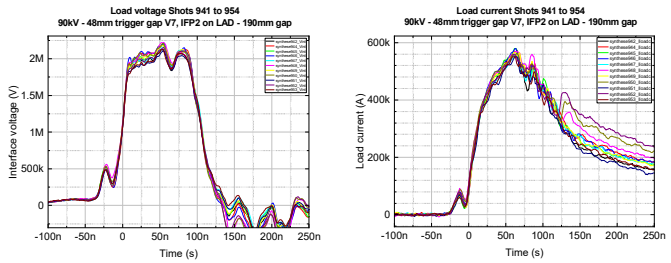

Fig. 9. Interface voltage and current on the load on 11 consecutive shots at 90kV w/o any refurbish

pulser. The Marx was detailed to take into account the closure times and ~140ns erection process based on [3]. The lines have been split in different sections according to the geometry. The oil switch was represented with the 3 gaps and with an inductance calculation based on the equation for a coaxial line using rods (depending on the arcs number on each gap). Finally we have added a Braginskii model for the diverter switch. This model stays in agreement with the initial evaluations and provides a very good fitting with the experimental results either on the resistive load or LAD. An integrated test campaign of the PFRP on the pulser has been done with AWE (28 shots completed at 80 and 90kV mainly) that showed a good operation of the pulser and good energy transfer to the diode (70-90kJ) with max. impedance of the diode ranging between 2 and 3 Ω, see [4].

VI. Conclusion

We have designed 'simple' generators, answering the requirements, which does not use any complex components (i.g. such as HV pressurized switches using laser triggering…). A compact design was obtained compared to older ones thanks to the use of a modern Marx, the suppression of the intermediate store and help of modern powerful electrostatic simulation software that probably allowed to reduce the margins. The use of a physical model for the switches (mainly the oil one) allowed providing reliable and predictive simulations. These HPP generators have been extensively mechanized to facilitate their operation and maintenance and improve the safety of personnel. Testing of the second machine have been completed at the end of 2021 and a new test campaign of the PFRP will be done with AWE in the 1st quarter of 2022 before delivery of the 2nd machine.

References

[1] F.Bayol et al, "Development and test of a high power conventional pulser for radiography application", in Proceedings of the EAPPC 2020, Biarritz

[2] John D. Shipman, "Design and performance of the new multi-channel oil output switch on the GambleIIA water dielectric pulse power generator at NRL", in Proceedings of the 3rd Pulse Power Conference, Albuquerque, 1981, pp. 475-477.

[3] B.Lassalle & al, "Analysis of the triggering behaviour of Marx generators using Spice simulations", in Proceedings of the 22nd Pulse Power Conference, Orlando, 2019.

[4] A.Jones et al, "Integration test of Plasma Filled Rod Pinch diode radiographic source", in Proceedings of the EAPPC 2020, Biarritz